

NMR study of the heavy-fermion alloy $\text{Ce}(\text{Cu}_{1-x}\text{Ni}_x)_2\text{Ge}_2$

N. Büttgen, R. Böhmer,* A. Krimmel,† and A. Loidl

Institut für Festkörperphysik, Technische Hochschule Darmstadt, D-64289 Darmstadt, Germany

(Received 12 October 1995)

A detailed ^{63}Cu NMR investigation is presented for the heavy-fermion system $\text{Ce}(\text{Cu}_{1-x}\text{Ni}_x)_2\text{Ge}_2$, focusing especially on the alloying induced transition from magnetic order to pure Kondo-like behavior. The broadening of the resonance line and the temperature dependence of the spin-lattice relaxation rate $1/T_1$ are studied in full detail. We provide experimental evidence for the appearance of heavy-fermion band magnetism for concentrations $x=0.6$ and $x=0.7$. For $x=0.8$ the spin-lattice relaxation rate $1/T_1$ follows a logarithmic temperature dependence which we interpret as a fingerprint of a non-Fermi-liquid behavior. Finally, $1/T_1$ is compared to the dynamic structure factor $S(\mathbf{Q},\omega)$ as determined in inelastic-neutron-scattering experiments.

I. INTRODUCTION

Despite the enormous progress that has been made in the knowledge of heavy-fermion systems (HFS),¹ many phenomena in these highly correlated electron systems are far from being fully understood. One of the issues of present interest is the behavior of HFS close to the borderline from the magnetic, RKKY-interaction dominated regime to the pure Kondo region.² Specifically, at this separation line non-Fermi-liquid behavior may appear due to the fact that the phase transition into a magnetically ordered state is pushed towards $T=0$ K and significant deviations in the susceptibility may show up.³ The easiest way to fine-tune the competing Ruderman-Kittel-Kasuya-Yosida (RKKY) and Kondo-like interactions is by changing the volume of the unit cell by alloying.

$\text{Ce}(\text{Cu}_{1-x}\text{Ni}_x)_2\text{Ge}_2$ is a well characterized heavy-electron system that reveals a transition from local-moment magnetism to a pure heavy-fermion behavior.⁴ CeCu_2Ge_2 reveals a characteristic Kondo-lattice temperature $T^*\approx 6$ K and undergoes a transition into a modulated magnetic structure with a partially Kondo-compensated moment at $T_N=4.1$ K.⁵ At hydrostatic pressures above 70 kbar magnetic order is suppressed and bulk superconductivity is induced.⁶ CeNi_2Ge_2 belongs to the class of nonmagnetic heavy Fermi-liquid systems with $T^*\approx 30$ K.⁷ In the mixed crystals, with increasing nickel concentration x the magnetic order changes and experimental evidence has been provided for the appearance of heavy-fermion band magnetism (HFMB) close to $x=0.5$.⁴ In heavy-fermion band magnets the spin degrees of freedom are transferred into the band states and a Stoner type of magnetism of the heavy quasiparticles is established.⁸ Finally, close to $x=0.75$ magnetic order is completely suppressed.⁴ A schematic x,T -phase diagram is presented in Fig. 1.

In this communication we report the results of a detailed NMR study of the ^{63}Cu spin-lattice relaxation in $\text{Ce}(\text{Cu}_{1-x}\text{Ni}_x)_2\text{Ge}_2$. Some preliminary results on CeCu_2Ge_2 have been reported earlier.⁹ In this work special emphasis is given to concentrations close to $x=0.75$, where magnetic order vanishes and the system passes into the pure Kondo regime. In addition we try to compare our NMR data

with neutron-scattering results of the dynamic structure factor given in Ref. 4.

II. MODEL CALCULATIONS

In order to derive a semiquantitative analysis of the temperature dependence of the spin-lattice relaxation rate $1/T_1$ in HFS, in the following we present some simplified calculations that take into account the most prominent and important interactions that will play a role in the compounds under consideration. Furthermore, these results should allow to elucidate the comparison of the NMR results with neutron data.

In addition to the Korringa relaxation rate that is usually observed in normal metals without localized magnetic moments, the experimental spin-lattice relaxation rate in HFS will be enhanced due to spin fluctuation effects. As suggested by Lysak *et al.*,¹⁰ we write

$$(T_1^{-1}) = (T_1^{-1})_K + (T_1^{-1})_f. \quad (1)$$

The Korringa relaxation represents the contribution to nuclear relaxation which originates from the contact interaction with conduction electrons and is given by¹¹

$$(T_1^{-1})_K = \pi \hbar^3 \gamma_e^2 \gamma_n^2 A_{\text{hf}}^2 N(E_F)^2 k_B T, \quad (2)$$

where A_{hf} is the transferred hyperfine coupling and $N(E_F)$ is the density of electronic states at the Fermi level. Hence, for HFS the Korringa relaxation may also provide an access to the hybridization-enhanced density of states at the Fermi level. The second term in Eq. (1) is due to spin fluctuations which will be transferred via the RKKY interaction from the local moments to the site of the NMR nucleus. It has been pointed out by Cox¹² that for nuclei with low atomic numbers the pure dipolar coupling may dominate the RKKY exchange.

From the fluctuation dissipation theorem the contribution $(1/T_1)_f$ for nuclear relaxation may be deduced:¹³

$$(T_1^{-1})_f = \frac{\gamma_n^2 k_B T}{2\mu_B^2} \sum_{\mathbf{Q}} |A_{\text{eff}}(\mathbf{Q})|^2 \frac{\text{Im}\chi(\mathbf{Q},\omega_0,T)}{\omega_0}. \quad (3)$$

The effective coupling between the localized f moment and the nucleus at site \mathbf{r} is given by

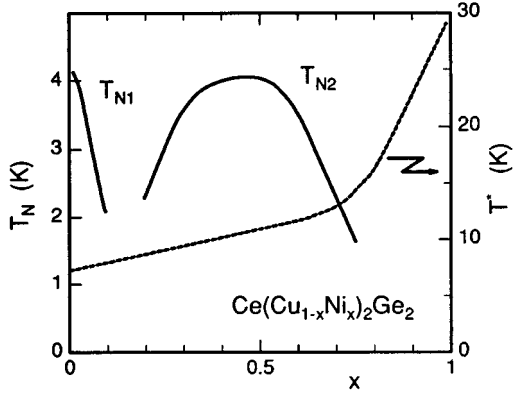


FIG. 1. x, T -phase diagram of $\text{Ce}(\text{Cu}_{1-x}\text{Ni}_x)_2\text{Ge}_2$, revealing two antiferromagnetic phases. Magnetic order is completely suppressed close to $x=0.75$. The evolution of the Kondo-lattice temperature T^* as a function of nickel concentration is shown by the dashed line.

$$A_{\text{eff}}(\mathbf{Q}) = \sum_j A_j(\mathbf{r}) \exp(i\mathbf{Q} \cdot \mathbf{r}). \quad (4)$$

A_{eff} will depend on the momentum transfer \mathbf{Q} and includes the coupling of the f spin to those of the conduction electrons and the form factors related to the hyperfine fields. Application of Eq. (3) requires a direct calculation of the absorptive part of the dynamic susceptibility $\text{Im}\chi(\mathbf{Q}, \omega_0, T)$ and of the effective hyperfine coupling A_{eff} . The probing copper nuclei are tetrahedrally coordinated by the $4f$ ions. Hence the calculation of A_{eff} would require one to sum over contributions from the four next-nearest cerium neighbors with a distance of 3.24 \AA . These calculations are beyond the scope of the present work.

Under the most naive assumption for this low number of nearest cerium atoms we neglect any \mathbf{Q} dependences. In this case Eq. (3) can be replaced by

$$(T_1^{-1})_f \propto \frac{k_B T}{\omega_0} \text{Im}\chi(\omega_0, T), \quad (5)$$

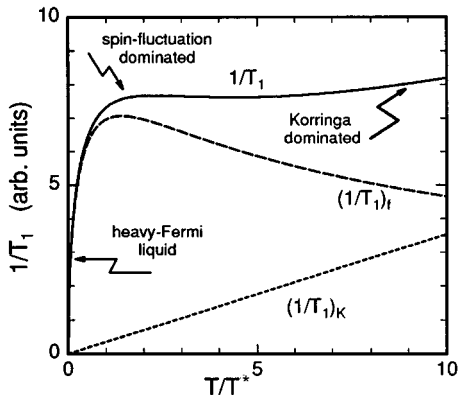


FIG. 2. Model calculation for the temperature dependence of the nuclear relaxation rate, according to Eq. (1). $T > T^*$: $\Gamma \propto \sqrt{T}$, $\chi_0 \propto C/(T + \sqrt{2}T^*)$; $T \leq T^*$: $\Gamma \approx \text{const}$, $\chi_0 \approx \text{const}$.

where ω_0 is the probing frequency of the NMR experiment. Furthermore we describe the absorptive part of the dynamic spin susceptibility by a purely relaxational *ansatz*

$$\text{Im}\chi = \chi_0 \frac{\omega\Gamma}{\omega^2 + \Gamma^2}. \quad (6)$$

Γ is the magnetic relaxation rate and χ_0 is the static susceptibility. Taking into account that the nuclear Larmor frequency $\omega_0 \ll \Gamma$, we can write

$$(T_1^{-1})_f \propto k_B T \frac{\chi_0}{\Gamma}. \quad (7)$$

In Fig. 2 a model calculation using Eq. (2) and Eq. (7) is shown. For $T > T^*$, χ_0 is the Curie-Weiss type static susceptibility with a Curie-Weiss temperature $\theta = \sqrt{2}T^*$.¹⁴ Following Cox *et al.*,¹⁵ a square-root dependence on temperature of the magnetic relaxation rate Γ has been used. For $T < T^*$, we assumed that the magnetic relaxation rate, as well as the static susceptibility are independent of temperature.

In neutron-scattering experiments the double-differential cross section measures the dynamic structure factor $S(\mathbf{Q}, \omega, T)$. For magnetic neutron scattering this scattering function is proportional to the imaginary part of the dynamic susceptibility¹⁷

$$S(\mathbf{Q}, \omega, T) = \frac{\text{Im}\chi(\mathbf{Q}, \omega, T)}{1 - \exp[-(\hbar\omega/k_B T)]}. \quad (8)$$

For temperatures $k_B T \gg \hbar\omega$, and again neglecting the \mathbf{Q} dependence Eq. (8) yields

$$S(\omega, T) \propto \frac{k_B T}{\hbar\omega} \text{Im}\chi(\omega, T). \quad (9)$$

With the relaxational susceptibility of Eq. (6) the dynamic structure factor is determined by a Lorentzian line centered at zero frequency. The linewidth is determined by the magnetic relaxation rate Γ and the area of the Lorentzian line by the static susceptibility χ_0 . On the basis of Eq. (5) and Eq. (9), the results of spin-lattice relaxation and neutron-scattering measurements for low energies are expected to trace one another, at least in the spin fluctuation regime where the Curie-Weiss type of the static susceptibility holds.

III. EXPERIMENTAL DETAILS AND RESULTS

The $\text{Ce}(\text{Cu}_{1-x}\text{Ni}_x)_2\text{Ge}_2$ samples were prepared by arc melting the stoichiometric quantities using $\geq 99.99\%$ pure constituent elements in an argon atmosphere. For the NMR experiment, the samples were crushed to powder, smaller in size than $40 \mu\text{m}$. After powdering, the samples were subjected to a further heat treatment for five days at $900 \text{ }^\circ\text{C}$. X-ray-powder diffraction showed that the samples were single phase with the ThCr_2Si_2 structure in the whole composition range. Increasing Ni concentration x at the copper site leads to a linear reduction of the volume of the unit cell, whereas the site symmetry at the copper probe remains undisturbed.

The samples were immersed into a paraffin matrix. With the exception of the $x=0.7$ sample, all measurements were performed on grain-oriented powder samples. Orientation

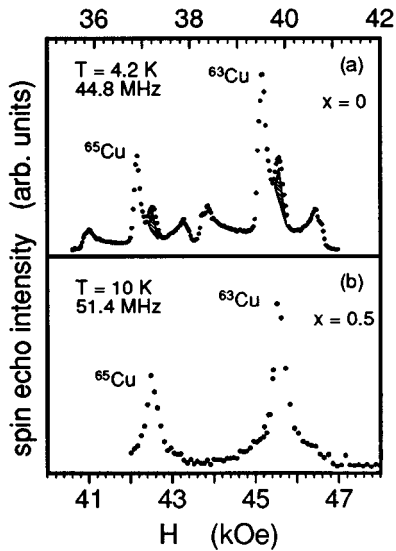


FIG. 3. Powder spectra of both copper isotopes taken at temperatures $T > T_N$. (a) Quadrupole split pattern of unoriented powder of CeCu_2Ge_2 . Results obtained after grain orientation are reported elsewhere (Ref. 9). The dashed peaks are due pick up of signal from elementary Cu in the radio frequency coil. (b) Powder pattern of $\text{Ce}(\text{Cu}_{0.5}\text{Ni}_{0.5})_2\text{Ge}_2$, where the quadrupole splitting is wiped out (see text).

procedure was achieved using a superconducting magnet (>5 T). The sample with the concentration $x=0.7$ has been measured unoriented, in order to show that the lack of quadrupole splitting of the Cu ($I=3/2$) powder pattern, which was observed for all nickel-doped samples, is not due to grain orientation. The NMR measurements were performed by a phase-coherent pulsed spectrometer in the temperature range from 1.6 to 180 K. Except for the measurements of the sample CeCu_2Ge_2 the radio frequency coil was made of silver. The spectra were measured by field sweeps using standard spin-echo detection ($\pi/2-\tau_D-\pi$, $\tau_D=70$ μs). In order to obtain the spin-lattice relaxation time T_1 , the echo train was augmented by a preceding inversion pulse being 20 μs long. The correct value of T_1 was obtained from a biexponential fit to the longitudinal nuclear magnetization recovery over four decades in time. The ratio of the biexponential decay rates of the excited central transition was given by the solution of the master equation for a nuclear spin system with $I=3/2$.¹⁸

Figure 3(a) shows the powder spectrum of CeCu_2Ge_2 . The spectrum is split due to first order quadrupole effects as expected for the symmetry ($4m2$) at the copper site.⁹ Second order shifts of the central transition are estimated to be about 25% of the observed linewidth, and therefore are beyond the resolution of the experiment. In contrast to the results in CeCu_2Ge_2 , all nickel doped samples reveal no quadrupole splitting of the powder pattern, although the site symmetry ($4m2$) at the copper probe is conserved. The absence of a quadrupole splitting is demonstrated for the $x=0.5$ sample in Fig. 3(b). The substitution of copper by nickel leads to a distribution of the charge density and hence to a corresponding distortion of the electrical field gradient (EFG) at the copper site. Obviously the nuclear quadrupole interaction with this distribution of EFG's wipes out the shift of the

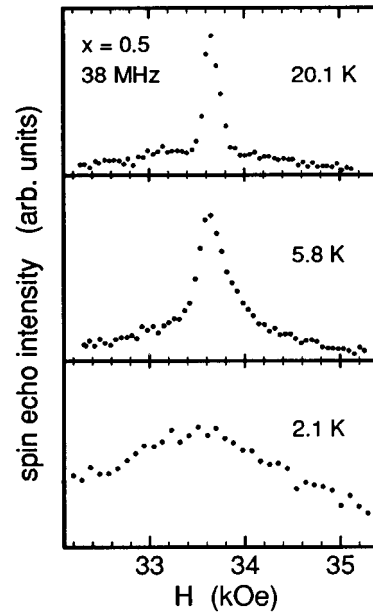


FIG. 4. ^{63}Cu resonance line shape in the paramagnetic and magnetically ordered phase of $\text{Ce}(\text{Cu}_{0.5}\text{Ni}_{0.5})_2\text{Ge}_2$ ($T_N \approx 4$ K).

satellite transitions. The single central transition of ^{63}Cu has been excited for the relaxation experiment.

The temperature dependence of the spectral line for $\text{Ce}(\text{Cu}_{0.5}\text{Ni}_{0.5})_2\text{Ge}_2$ is shown in Fig. 4 and reveals a drastic broadening of the resonance line for temperatures $T < T_N$. This behavior results from an inhomogeneous broadening due to an incommensurate magnetic order (IC) as has been established by neutron-scattering experiments.⁴ Due to the IC structure the copper sites experience a wide distribution of transferred hyperfine fields resulting in a broad resonance line. The temperature dependence of the full width at half maximum (FWHM) of the resonance line for several nickel concentrations x is shown in Fig. 5. For $x=0$ and $x=0.5$ the linewidths strongly increase below $T_N \approx 4$ K. However, already for the sample with $x=0.6$ with a magnetic phase transition temperature close to 3.5 K, the linewidth remains almost constant, similar to the behavior in the nonmagnetic compound with $x=0.8$. This behavior could indicate a transition into the regime of HFBM or it signals an almost fully

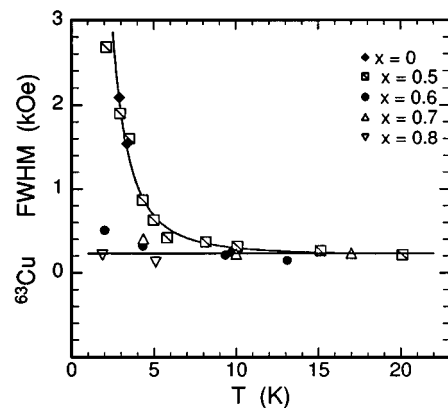


FIG. 5. ^{63}Cu linewidth (FWHM) vs temperature T in $\text{Ce}(\text{Cu}_{1-x}\text{Ni}_x)_2\text{Ge}_2$. The lines are drawn to guide the eye.

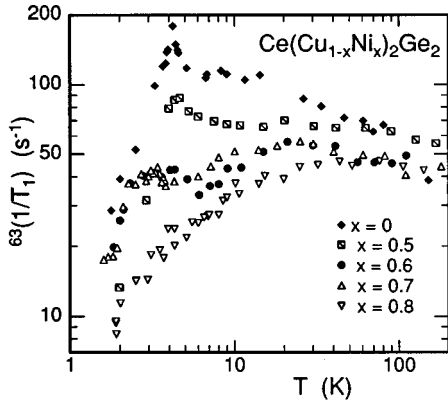


FIG. 6. Spin-lattice relaxation rate ${}^{63}(1/T_1)$ vs temperature T in $\text{Ce}(\text{Cu}_{1-x}\text{Ni}_x)_2\text{Ge}_2$.

Kondo compensation of the ordered moments. And indeed, in neutron diffraction experiments, no indications of magnetic Bragg reflections could be detected in $\text{Ce}(\text{Cu}_{0.35}\text{Ni}_{0.65})_2\text{Ge}_2$. From the nonobservability of the magnetic reflection an upper bound of $0.2\mu_B$ has been estimated for the ordered moment.⁴

Figure 6 shows the temperature dependence of the ${}^{63}\text{Cu}$ spin-lattice rate $1/T_1$ on a double logarithmic scale. For $T \geq 10$ K all relaxation rates reveal only weak temperature dependences. This observation suggests the dominance of RKKY type interactions which are transferred via hyperfine coupling to the copper nuclei and provides experimental evidence for the spin-fluctuation regime (see Fig. 2). Figure 6 nicely documents the increasing compensation of the ordered moment with increasing x (at $T = 10$ K, $1/T_1$ decreases by a factor of 4 when x is increased from $x = 0$ to $x = 0.8$). For concentrations $0 \leq x \leq 0.7$, anomalies in $1/T_1$ reveal clear evidence for the onset of magnetic order at low temperatures. The anomalies are rather sharp for $x \leq 0.5$, but are rounded for $x = 0.6$ and $x = 0.7$. The strong increase of $1/T_1$ in CeCu_2Ge_2 close to T_N possibly originates from critical spin fluctuations close to T_N .⁹ For $x = 0.8$, the relaxation rate continuously decreases for $T \leq 40$ K. It is important to note that $1/T_1$ vs T for $x = 0.8$ never reveals a linear dependence, as it is expected for a pure heavy-Fermi liquid.

To elucidate this behavior in more detail, the spin-lattice relaxation rate for $x = 0.7$ and $x = 0.8$ are shown in a semi-logarithmic representation (Fig. 7). For comparison with theoretical predictions we plotted $1/T_1$ vs $\log_{10} T$ [Fig. 7(a)] as well as $1/T_1 T$ vs $\log_{10} T$ [Fig. 7(b)]. According to Eq. (5), $(T_1 T)^{-1}$ corresponds to the dynamic susceptibility if Korringa processes can be neglected. It is evident that the spin-lattice relaxation time for $\text{Ce}(\text{Cu}_{0.2}\text{Ni}_{0.8})_2\text{Ge}_2$ reveals a logarithmic temperature dependence over one decade in temperature. An extension of these measurements to even lower temperatures would be highly desirable. The experimental results for $x = 0.7$ reveal the onset of moment compensation for $T \approx 20$ K (maximum value in $1/T_1$) and a magnetic phase transition close to 2.5 K. We interpret this magnetic phase transition deep in the Kondo-compensated regime as a clear signature of HFBM.

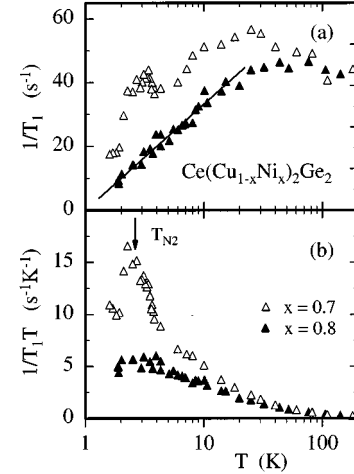


FIG. 7. (a) Spin-lattice relaxation rate ${}^{63}(1/T_1)$ vs temperature T for $x = 0.7$ and $x = 0.8$ samples. The line indicates a logarithmic temperature dependence. (b) Absorptive part of the dynamic susceptibility $\text{Im}\chi(\omega_0, T) \propto 1/T_1 T$ according to Eq. (5).

IV. ANALYSIS AND DISCUSSION

A. Comparison with inelastic-neutron-scattering experiments

In this section we compare the present NMR results with results as obtained by inelastic-neutron-scattering experiments.^{4,5} Figure 8 shows the spin-lattice relaxation rate (closed symbols) for $x = 0$ (a), $x = 0.5$ (b), $x = 0.6$ (c), and $x = 0.8$ (d) in double-logarithmic representations. These NMR results are compared with the temperature dependence of the dynamic structure factor $S(\mathbf{Q}, \omega)$ as determined at a measuring frequency $\nu = 240$ GHz in inelastic-neutron-scattering experiments (open symbols):^{4,5} $x = 0$ (a), $x = 0.5$ (b), $x = 0.6$ (c), and $x = 1$ (d). In these experiments a summation over \mathbf{Q} has been obtained by using polycrystalline samples and time-of-flight techniques.

At first glance the overall agreement of the spin-lattice relaxation time and the dynamic structure factor is astonishingly good. Figure 8 reveals that the temperature dependence

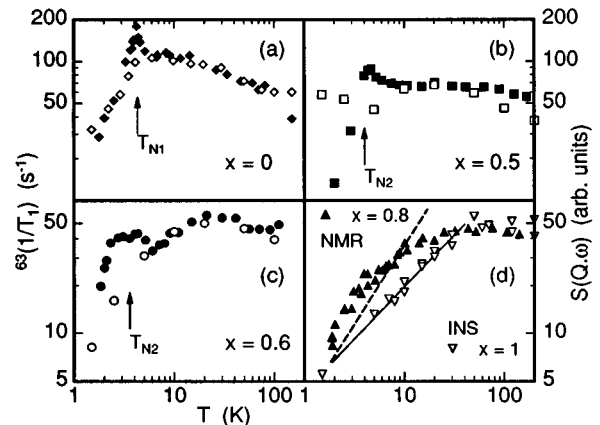


FIG. 8. Comparison of nuclear relaxation rate $1/T_1$ (closed symbols) and scattering amplitude $S(\mathbf{Q}, \omega)$ (open symbols) from inelastic neutron scattering ($\hbar\omega_0 = 0.3\text{meV}$). (d) The dashed and solid lines indicate power law dependences with exponents 1 and $2/3$, respectively.

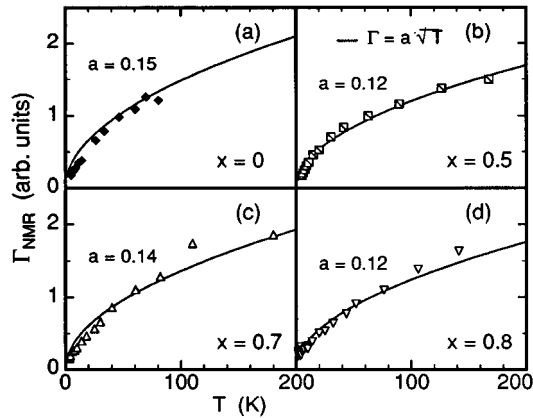


FIG. 9. Magnetic relaxation rate derived from NMR measurement $\Gamma_{\text{NMR}} \propto T_1 T \chi_0$. The solid lines were calculated using a square-root dependence of the magnetic relaxation rate.

of the dynamic susceptibility scales for all frequencies $\nu < 250$ GHz and for $T > T_N$. Significant deviations appear for $T < T_N$. For $x=0$ both techniques, which operate on vastly different frequency scales, detect the opening of a gap in the magnetic excitation spectrum. This is indicated by the strong decrease of $1/T_1$, as well as of $S(\mathbf{Q}, \omega)$ below T_N . However, already for $x=0.5$ a spin gap opens on the frequency scale of the NMR experiment (closed symbols), but not at the GHz frequencies as probed by neutron scattering (open symbols). For $x=0.6$ [Fig. 8(c)] both data sets signal the transition into a heavy-fermion regime for $T \leq 20$ K. However, strong spin fluctuations dominate the spin-lattice relaxation rate which are suppressed for $T < T_N$. The dynamic structure factor decreases continuously towards low temperatures and reveals the presence of a strong on-site Kondo effect suppressing all intersite fluctuations at the cerium site. This indicates that strong hybridization yields a strongly enhanced density of electronic states at the f site, but RKKY-type interactions can still be detected at the copper site. We speculate that $x=0.6$ represents the borderline between the magnetism of localized moments and HFBM.

Finally, Fig. 8(d) shows the results for samples in the fully established Kondo regime. For $T < 30$ K and decreasing temperatures $1/T_1$ and $S(\mathbf{Q}, \omega)$ both exhibit a continuous decrease. However, as has been demonstrated in Fig. 7, the spin-lattice relaxation rate follows a logarithmic temperature dependence, while the dynamic structure factor for $x=1$ can be described by a power-law behavior $S(\mathbf{Q}, \omega) \propto T^\alpha$, with $\alpha \approx 2/3$ [solid line in Fig. 8(d)]. For a pure Fermi liquid both quantities should depend linearly on temperature. To demonstrate that the deviations from Fermi-liquid behavior are indeed significant, the dashed line in Fig. 8(d) indicates a linear temperature dependence.

Using the experimentally observed spin-lattice relaxation rate and the static susceptibilities¹⁹ of $\text{Ce}(\text{Cu}_{1-x}\text{Ni}_x)_2\text{Ge}_2$ we calculated the magnetic relaxation rate Γ_{NMR} on the basis of Eq. (7). The results are shown in Figs. 9(a)–9(d), where Γ_{NMR} is plotted as a function of temperature. For high temperatures $\Gamma_{\text{NMR}}(T)$ closely follows a square-root dependence as theoretically predicted by Cox *et al.*¹⁵ The prefactor a depends on the degeneracy of the ground multiplet and on $(\sqrt{T^*})^{-1}$.¹⁵ In the concentration region investigated T^* in-

creases almost by a factor of 2 (see Fig. 1). Hence a should decrease continuously from 0.15 ($x=0$) to 0.11 ($x=0.8$), a behavior which is only roughly resembled in Fig. 9. For temperatures $T < T^*$ a temperature-independent residual linewidth is expected for a $S=1/2$ Anderson model theoretically.¹⁶ The observed linear temperature dependence of Γ_{NMR} at low temperatures deviates from the theoretically expected finite residual relaxation rate.^{15,16} This deviation most likely stems from a distribution of crystal field levels which originate in the site disorder of the nickel and copper ions.

B. Non-Fermi-liquid behavior

Finally we want to comment in more detail on the temperature dependence of the dynamic susceptibility in $\text{Ce}(\text{Cu}_{1-x}\text{Ni}_x)_2\text{Ge}_2$ for $x=0.8$ and $x=1$ as shown in Fig. 7 and Fig. 8(d). Theoretically non-Fermi-liquid behavior is expected to occur close to a quantum phase transition,²⁰ but can also occur in multichannel Kondo systems²¹ or in impurity systems.²² In the former two cases the bulk susceptibility is expected to behave according to $\chi(T) \propto C(T)/T \propto -\ln(T/T^*)$. In disordered Kondo systems the low-temperature thermodynamics also deviate from a Fermi-liquid behavior and are characterized by a diverging susceptibility and a specific heat rising faster than T . Theoretically the scaling relation between the static and the dynamic susceptibilities has yet to be established. Preliminary results reveal that the spin-lattice relaxation rate follows a $1/T_1 \propto T^{0.3} \ln(T/T^*)$ dependence assuming a logarithmic divergence of the Sommerfeld coefficient $\gamma = C/T$.²³ We believe that the temperature-independent linewidth for $\text{Ce}(\text{Cu}_{0.2}\text{Ni}_{0.8})_2\text{Ge}_2$ (see Fig. 5) provides evidence against Kondo disorder.²⁴

The dynamic structure factor $S(\mathbf{Q}, \omega)$ in CeNi_2Ge_2 follows a power-law behavior, but with an exponent $\alpha \approx 2/3$ which is significantly below the value of unity as expected for a Fermi liquid. It is interesting to note that in this compound also the Sommerfeld coefficient $\gamma(T)$ increases continuously with decreasing T and zero field results could not be explained with an $S=1/2$ impurity Kondo model. Clearly more experimental and theoretical work is needed to elucidate the non-Fermi-liquid behavior in $\text{Ce}(\text{Cu}_{1-x}\text{Ni}_x)_2\text{Ge}_2$.

V. SUMMARY AND CONCLUSION

We have presented a detailed NMR investigation of the heavy-fermion system $\text{Ce}(\text{Cu}_{1-x}\text{Ni}_x)_2\text{Ge}_2$ where the pure compounds reveal local-moment magnetism ($x=0$) and a nonmagnetic, heavy-fermion ground state ($x=1$). The concentrations $x=0, 0.5, 0.6, 0.7,$ and 0.8 have been investigated. For all compounds, we measured the temperature dependence of the resonance line and of the spin-lattice relaxation rate.

From these experiments we conclude that the samples with concentrations $0 \leq x \leq 0.5$ are characterized by local-moment magnetism. The compounds with $x=0.6$ and 0.7 belong to the class of heavy-fermion band magnets. This conclusion is drawn because the magnetic phase transition in these samples develops deep in the Kondo-compensated re-

gime. Finally, $\text{Ce}(\text{Cu}_{0.2}\text{Ni}_{0.8})_2\text{Ge}_2$ reveals a logarithmic increase of the spin-lattice relaxation rate indicative for non-Fermi-liquid behavior.

In addition we presented a detailed comparison of the spin-lattice relaxation rate with the dynamic structure factor as determined in inelastic-neutron-scattering experiments. The calculation of the magnetic relaxation rate using results from NMR and bulk susceptibility measurements reveals a

square-root dependence at high temperatures, but an almost linear dependence on temperature for $T \rightarrow 0$.

ACKNOWLEDGMENTS

We are grateful to F. Fischer for help with sample preparation. This work was supported by the Deutsche Forschungsgemeinschaft within Sonderforschungsbereich 252.

*Permanent address: Institut für Physikalische Chemie, Johannes Gutenberg-Universität, D-55099 Mainz.

†Permanent address: BENSC, Hahn-Meitner Institut, D-14109 Berlin.

¹N. Grewe and F. Steglich, *Handbook on the Physics and Chemistry of Rare Earths* (Elsevier Science B.V., Amsterdam, 1991), Vol. 14.

²S. Doniach, *Physica B* **91**, 231 (1977).

³C.L. Seaman, M.B. Maple, B.W. Lee, S. Ghamaty, M.S. Torikachvili, J.-S. Kang, L.Z. Liu, J.W. Allen, and D.L. Cox, *Phys. Rev. Lett.* **67**, 2882 (1991); B. Andraka and G.R. Stewart, *Phys. Rev. B* **47**, 3208 (1993); H. v. Löhneysen, *Physica B* **206&207**, 101 (1995); B. Bogenberger and H. v. Löhneysen, *Phys. Rev. Lett.* **74**, 1016 (1995).

⁴A. Loidl, A. Krimmel, K. Knorr, G. Sparn, M. Lang, C. Geibel, S. Horn, A. Grauel, F. Steglich, B. Welslau, N. Grewe, H. Nakotte, F.R. de Boer, and A.P. Murani, *Ann. Phys.* **1**, 78 (1992).

⁵G. Knopp, A. Loidl, K. Knorr, L. Pawlak, M. Duczmal, R. Caspary, U. Gottwick, H. Spille, F. Steglich, and A.P. Murani, *Z. Phys. B Condens. Matter* **77**, 95 (1989).

⁶D. Jaccard, K. Behnia, and J. Sierro, *Phys. Lett. A* **163**, 475 (1992).

⁷G. Knopp, A. Loidl, R. Caspary, U. Gottwick, C.D. Bredl, H. Spille, and F. Steglich, *J. Magn. Magn. Mater.* **74**, 341 (1988).

⁸N. Grewe and B. Welslau, *Solid State Commun.* **65**, 437 (1988); N. Grewe, *ibid.* **66**, 1053 (1988).

⁹N. Büttgen, R. Böhmer, and A. Loidl, *Solid State Commun.* **93**, 753 (1995).

¹⁰M.J. Lysak and D.E. MacLaughlin, *Phys. Rev. B* **31**, 6963 (1985).

¹¹C.P. Slichter, *Principles of Magnetic Resonance* (Springer, New York, 1990).

¹²D.L. Cox, *Phys. Rev. B* **35**, 6504 (1987).

¹³C.H. Pennigton and C.P. Slichter, in *Physical Properties of High Temperature Superconductors II*, edited by D.M. Ginsberg (World Scientific, Singapore, 1990).

¹⁴J. Callaway, *Quantum Theory of the Solid State* (Academic, New York, 1991), p. 448.

¹⁵D.L. Cox, N.E. Bickers, and J.W. Wilkins, *J. Appl. Phys.* **57**, 3166 (1985).

¹⁶D.L. Cox (private communication).

¹⁷M. Loewenhaupt and K.H. Fischer, *Handbook on the Physics and Chemistry of Rare Earths* (Elsevier Science B.V., Amsterdam, 1992), Vol. 16.

¹⁸E.R. Andrew and D.P. Tunstall, *Proc. Phys. Soc.* **78**, 1 (1961).

¹⁹U. Habel, Diploma thesis, TH Darmstadt, 1988.

²⁰A.J. Millis, *Phys. Rev. B* **48**, 7183 (1993).

²¹For a review, see P. Schlottmann and P.D. Sacramento, *Adv. Phys.* **42**, 641 (1993); T.-S. Kim and D.L. Cox, *Phys. Rev. Lett.* **75**, 1622 (1995).

²²R.N. Bhatt and D.S. Fisher, *Phys. Rev. Lett.* **68**, 3072 (1992); V. Dobrosavljevic, T.R. Kirkpatrick, and G. Kotliar, *ibid.* **69**, 1113 (1992).

²³M. Continentino (private communication).

²⁴O.O. Bernal, D.E. MacLaughlin, H.G. Lukefahr, and B. Andraka, *Phys. Rev. Lett.* **75**, 2023 (1995).